TSINGHUA SCIENCE AND TECHNOLOGY
ISSN 1007-0214 13/20 pp1785–1795
DOI: 10.26599/TST.2023.9010119
Volume 29, Number 6, December 2024

Intelligent Transportation System Performance Analysis of Indoor and Outdoor Internet of Vehicle (IoV) Applications towards 5G

Preeti Rani and Rohit Sharma*

Abstract: The Internet of Vehicles (IoVs) has seen rapid development due to advances in advanced communication technologies. The 5-th Generation (5G) systems will be integrated into next-generation vehicles, enabling them to operate more efficiently by cooperating with the environment. The millimeter Wave (mmWave) technology is projected to provide a large bandwidth to meet future needs for more effective data rate communications. A viable approach for transferring raw sensor data among autonomous vehicles would be to use mmWave communication. This paper attracts various research interests in academic, indoor, and outdoor mmWave operations. This paper presents mmWave propagation measurements for indoor and outdoor at 66 GHz frequency for IoVs scenarios. The proposed model examines the equivalent path loss using Free-Space Path Loss (FSPL) based on the transmitter and receiver distances for indoor and outdoor communications of the vehicles. In the indoor scenario, path loss propagation has the lowest penetration loss, but it is ineffective in the outdoor scenario because distance increases as free space path loss increases. The probability of error is increased, concerning the transmitter and receiver distances due to propagation effect, packet collisions, busy receiver, and sensing threshold. The proposed methodology shows a higher packet delivery ratio and average throughput with less delay in the connection during transmission.

Key words: Free-Space Path Loss (FSPL); Internet of Vehicles (IoVs); millimeter Wave (mmWave); the 5-th Generation (5G); indoor communication; outdoor communication

1 Introduction

According to the extensive spectrum bandwidth accessible for wireless communications, the millimeter Wave (mmWave) frequency bands have recently attracted much attention. The spectrum bandwidth should support significant capacity growth in the next generation (the 5-th Generation (5G)) cellular system. A successful method of combating high-frequency propagation loss is essential to the practicality of mmWave mobile communications[1].

Due to their low-latency requirements and wideband capability, Vehicle-to-Vehicle (V2V) communication will largely depend on mmWave networks in the coming years. The V2V channel-sounding campaigns were mostly restricted to frequencies below 6 GHz in various scenarios (parking garage, urban, highway, suburban, and intersections). Compared to inter-vehicle communication standards based on IEEE 802.11p, 5G technologies offer a new paradigm for connecting vehicles with high-speed data. 5G communication features are highly conducive to vehicle positioning due to their particular signal characteristics. The mmWave refers to electromagnetic (radio) waves with a 30–300 GHz frequency range. The formula $\lambda = c/f$

• Preeti Rani and Rohit Sharma are with Department of Electronics and Communication Engineering, Faculty of Engineering and Technology, SRM Institute of Science and Technology, Ghaziabad 201204, India. E-mail: preetiresearcher1@gmail.com; rohitapece@gmail.com.
* To whom correspondence should be addressed.
Manuscript received: 2023-07-25; revised: 2023-09-23; accepted: 2023-10-12

can be used to compute the wavelength of electromagnetic radiation, with speed of light $c = 3 \times 10^8$ m/s, and frequency f. The wavelength range of the mmWave band is 10 mm at 30 GHz and 1 mm at 300 GHz[2].

Recently, developments in the Internet of Things (IoT) domain impacted Vehicle Ad-hoc Networks (VANETs), now called the Internet of Vehicle (IoV). Intelligent Transportation Systems (ITS) applications require very low latency, significantly lower than existing communication networks. The V2V and Vehicle-to-Infrastructure (V2I) communication for connected vehicles is expected to be an extremely large data transmission. As a result, the most pressing issue for current wireless networks is that they require significantly more data than in the past, causing the radio-frequency spectrum below 6 GHz to become overloaded. The service is slower, and more connections are dropped due to the limited bandwidth. As a result, the mmWave spectrum is being examined for next-generation wireless networks, or 5G, which might offer 10 times the bandwidth and capacity of cellular networks[3].

Furthermore, academic and commercial research[4, 5] has reported the possibility of mobile broadband networks operating at frequencies higher than 6 GHz. It is worth mentioning that the allowed spectrum of 3.5 GHz could be assigned for 5G applications in frequency bands lower than 6 GHz[6]. According to much research, the 3.5 GHz frequency band is the direct access connection for indoor communication, but the 28 GHz frequency band can be utilized as a backhaul connection.

Other studies investigate the outdoor to indoor propagation channel at various mmWave frequencies. Table 1 compares indoor and outdoor frequency, bandwidth, distance, and propagation models. As vehicular communication is application-oriented, the authors proposed a strategy that lets vehicles distinguish selfishness through the value-based assessment of messages[19]. IoVs are a modern form of IoT, allowing vehicles to communicate and provide different mobile applications, allowing vehicles to be intelligent. Benalia et al.[20] examined IoV data dissemination based on 5G communication technologies, architecture, services, and challenges. In outdoor scenarios, Multiple Input Multiple Output (MIMO) and Distributed Antenna System (DAS) technologies are used for long-distance communications at sub-6 GHz frequency bands. At wireless Indoor Access Points (IAPs), mmWave and beamforming communication technologies provide high-speed services within short distances for indoor users[21]. The various existing research based on indoor and outdoor communication is presented in Table 2.

A smart automobile makes that time safer, more

Table 1 Comparative study for indoor and outdoor environment.

Reference	Environment	Frequency (GHz)	Bandwidth	Distance (m)	Performance study
[7]	Indoor	38–65	1000 MHz	1–40	Root-Mean-Square (RMS) delay spread, path loss versus distance
[8]	Outdoor	28 and 38	400 MHz	50–200	Path loss, Close-In-Frequency (CIF)
[9]	Outdoor	32	1 GHz	1–141	Path loss and efficiency
[10]	Outdoor	15 and 28	200 MHz	20–190	Signal strength (dBm), efficiency
[11]	Indoor	38 and 42	500 MHz	1–50	Delay sequence, path loss, and received power
[12]	Indoor	28, 38, 60, and 73	40 MHz	2–67	Average user throughput, spectral efficiency, and fairness index
[13]	Outdoor to indoor	3.5, 4.9, and 28	100 MHz	1–20	Path loss versus Transmitter-Transmitter (Tx-Tx) separation, antenna performance
[14]	Indoor to outdoor	30–300	5.9 GHz	1–40	Path loss, Spectral Efficiency (SE)
[15]	Outdoor	28 and 73	1 GHz	50–500	Delay, transmission power, Road Side Unit (RSU), and vehicle performance
[16]	Indoor and outdoor	28 and 73	5.9 GHz	1–500	Throughput, delay, and packet loss
[17]	Indoor and outdoor	60	Narrowing bandwidth from 90° to 45°	100–500	Packet Delivery Ratio (PDR), latency, and throughput
[18]	Indoor and outdoor	66	5.9 GHz	100–400	Latency and throughput

Table 2 Survey on mmWave technique.

Reference	MIMO system and RF chain	Methodology	Phase Shifters (PS) and Radio Frequency (RF) chains	Application area, Frequency Division Duplex (FDD)/Time Division Duplex (TDD)	Channel type	Effect on performance metric
[22]	Tx = 128, $N_{RF} = N_{user} = 4$	Multi-User Multiple Input Multiple Output (MU-MIMO) system with phased zero forcing.	RF chains, i.e., $N_{RF} = N_{user}$	MmWave massive MIMO TDD	mmWave channels with Rayleigh fading and sparse scatter	RF hardware with low complexity, SE of 1 dB less than zero-forcing precoding with full complexity.
[23]	$N_t = 64$, $N_{user} = 16$, single antenna user	A novel method is proposed to reduce the N_t^{RF} and PS. A scheduling procedure is presented for $N_t^{RF} <$ Rank of digital precoder	N_t^{RF} = Rank of digital precoder, $N_p = 20 - 40$	Microwave as well as mmWave	Frequency selective & Rayleigh fading channel model	Convenient for practical application & performance, better than existing in both frequency selective as well as flat fading channel.
[24]	Tx = 32, 64, $N_{user} = 12$, $N_{RF} = 1, 2, 4, 8, 16, 32, 64$	An optimization problem is resolved iteratively instead of Semi Definite Relaxation (SDR).	N_t^{RF} = constant for N_p = 1, 2, 4, 8, 16, 32, 64, PS=2 bits resolution	Massive MIMO, as well as mmWave systems	Gaussian channel model	Performance is close to full digital beamformer with less number of RF chains. As N^{RF} increases, transmitted power decreases.
[25]	64×16 MIMO system, $N_{RF} = 6$	Three algorithms for Point to Point (P2P) and MU-MISO. For P2P $N^{RF} > 2N_s$. If the first condition is not satisfied, then, $N^{RF} = N_s$. Within finite resolution PS and $N_s < N^{RF} < 2N_s$ with finite resolution PS.	Infinite/finite PS is utilized. $N^{RF} = 2N_s$	Significant P2P Multi-User Multi Input Single Output (MU-MISO) & MIMO, TDD is used.	Geometric channel	A fully Digital Beamforming (DB) system would approximate coverage capacity and spectral efficiency.
[26]	16×16 Uniform Planar Array (UPA), 256×1 Uniform Linear Array (ULA), $N_{RF} = 64$	A novel Spatial Channel (SC) and Hybrid Beamforming (HB) technique is proposed.	Reduced PS $N_t^{RF} = 64$	Significant P2P MU-MISO & MIMO, TDD is used	3D geometrically statistical channel model	Multiple user groups can be served, beamforming is highly directive, and power consumption is low.
[27]	64×8 MIMO system, $N_{RF} = 1$	The RF-extended HB architecture can realise any Full Duplex (FD).	Two PS on a single RF	Massive MIMO, TDD	Directional Vector (DV) channel model	Ensure optimal performance.
[28]	64×64 MIMO system, $N_{RF} = 1$	HB optimization for low-resolution PS based on codebooks.	For P2P MIMO, $N^{RF} = N_s$, for MU-MIMO, N^{RF}= number of users	P2P mmWave MIMO system, TDD	Geometric channel model	A low-resolution PS will reduce power consumption, and a polynomial complexity will increase SE.
[29]	Tx = 128, $N_{user} = 4$, $N_{RF} = 4$	QR decomposition is used to partition a fully digital presidency into two matrices.	$N_t^{RF} = 4$, the sum of two PS is used to define every entry of Analog Beamforming (AB)	TDD, massive MIMO	Practical & Rayleigh fading channel model	The performance is comparable to full digital with less RF chain.
[30]	Tx = 16, 32, 64, 128, $N_{user} = 4, 8, 16, 32$, $N_{RF} = 4, 8, 16, 32$	To maximize capacity with low complexity, MU-MIMO uses phased zero-forcing.	$N_t^{RF} = N_u$	5G frequency band with TDD	Rician, Rayleigh, Nakagami-m channel model	The RF chain is reduced, and the performance is comparable to a full digital.

(to be continued)

Table 2 Survey on mmWave technique. (continued)

Reference	MIMO system and RF chain	Methodology	Phase Shifters (PS) and Radio Frequency (RF) chains	Application area, Frequency Division Duplex (FDD)/Time Division Duplex (TDD)	Channel type	Effect on performance metric
[31]	Tx = 128, N_{user} = 8, N_{RF} = 16	HB design for mulit-user MIMO.	RF chain and PS are both on the transmitter and receiver side.	Massive MIMO TDD, MU-MIMO	Rayleigh fading channel model	The HB design scheme outperforms Base Station (BS) equipped with large or small antenna arrays.

efficient, more fun, pollution-free, and affordable. Maintaining the optimum use of resources and addressing rising needs is challenging due to the increasing popularity of vehicle users and the diversity of service requests. Therefore, VANET will require modernized working practices in the future. Innovative communication technologies are used to create intelligent transportation management systems and driver assistance systems. Automobiles and road infrastructure can communicate entertainment and traffic information over vehicular ad-hoc networks to improve transportation effectiveness, accident prevention, and pedestrian comfort[32]. For V2I communication systems characterized by the high mobility of mobile users, we propose a data-aided channel tracking scheme using lens antenna arrays and millimeter wave channels with spatial sparsity[33]. Sejan and Chung[34] developed an MIMO VLC system capable of connecting IoT devices to achieve long-range indoor communication. This study proposes an MIMO VLC monitoring system to monitor particulate matter, temperature, and humidity indoors. Experimental trials analyze the error performance of four different single-carrier techniques. The maximum communication range is then evaluated in order to ensure efficient network planning and uninterrupted connectivity[34]. Communication issues related to V2I applications can be solved using the 5G mmWave.

Nevertheless, 5G mmWave still needs to be evaluated for vehicular communication in urban and indoor-outdoor scenarios. An assessment of the performance of 5G mmWave based vehicular communications in such traffic scenarios is presented in this study. This paper focuses on the indoor and outdoor performance analysis for IoV applications towards 5G. This architecture will improve data broadcasting using promising and effective transmission technologies such as Software-Defined Network (SDN) functionality, 5G network properties, and cloud-based computing. We develop a generic 5G-based IoV architecture called IoVs based on 5th-generation communication.

(1) The paper observes the real-world performance of the IoVs with the mmWave transmitter and receiver for indoor and outdoor communication.

(2) The mmWave transmitter and receiver model using IEEE 802.11p V2V and V2I communications is used to assure optimal real-time performance of communication signal strength, packet delivery, and loss ratio.

(3) The performance of mmWave transmitters and receivers at 66 GHz carrier frequency with different path losses according to indoor and outdoor communication is investigated in this work.

(4) With mmWave technologies, RF communication has been considered to facilitate vehicle applications in the IoVs.

The paper is organized as follows. Introduction and related work are explained in Section 1. The proposed methodology and simulation design are presented in Section 2. The numerical simulation and result investigation are presented in Section 3 with the proposed, designed model and graphical representation of the performance of the IoVs system. Section 4 describes the conclusion.

2 Methodology

2.1 System model

This paper demonstrates the proposed methodology for modelling and simulating a 66 GHz Quadrature Phase Shift Keying (QPSK) RF transmits and receives system for the IoVs, as mentioned in Fig. 1. The system has RF imperfections, transmit array radiation effects, a

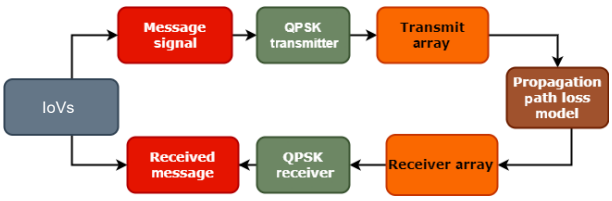

Fig. 1 System model of the proposed work.

narrowband receive array, and a baseband receiver with system impairment modifications and message decoding. The antenna beamforming direction is well-defined using azimuth and elevation angles, and it is computed in the RF receive antenna using a root MUSIC Direction of Arrival (DoA) algorithm.

The RF transmitter array configuration is divided into three parts due to the system's versatility and the separation of signals across different frequency bands: RF transmitter cell, Intermediate Frequency (IF)/Local Oscillator (LO), and power supply. The RF transmitter setup is depicted in Fig. 2. First, the IF chain signal is amplified. RF signals are created by mixing the IF signal with the LO signal. Long-distance transmission requires amplification of the RF signal by a power amplifier. Each RF receiver channel uses a superheterodyne technique. Front-end components include a Power Amplifier (PA), antenna array, LO power amplifier, upconverter, IF signal amplifier, and LO powder divider.

The receiver system comprises RF receiver cell modules, IF/LO modules, and a power supply module. The RF receiver arrays have a similar procedure as the transmitter array. As shown in Fig. 3, each RF receiver

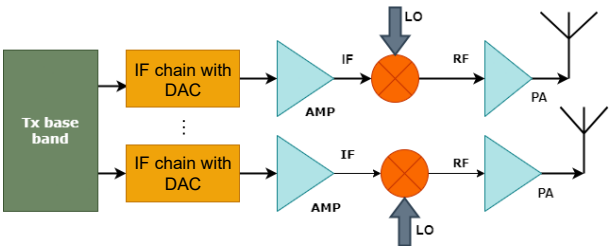

Fig. 2 RF mmWave transmitter model.

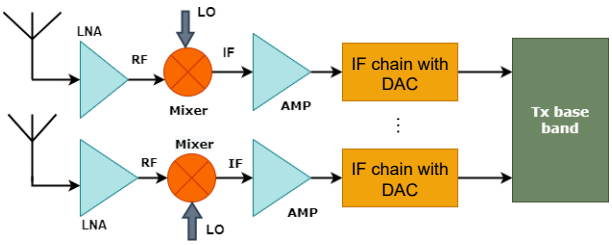

Fig. 3 RF mmWave receiver model.

channel used a superheterodyne method. The front end of the receiver model contains the Low-Noise Amplifier (LNA), patch antenna array, down converter, LO power amplifier, LO powder divider, and IF signal amplifier.

We first consider a P2P large-scale MIMO system in which a BS with N antennas transmit N_s data symbols to an IoV with M antennas where $\min(n,m)'' N_s$. The number of RF chains transmitting and receiving, i.e., $N_t^{\mathrm{RF}} = N_r^{\mathrm{RF}} = N^{\mathrm{RF}}$ is assumed to be the same without loss of generality. The simplified equation of the spectral efficiency rate R is mentioned in Eq. (1).

$$R = \log_2 \left| I_M + \frac{1}{\sigma^2} W_t \left(W_t^{\mathrm{H}} W_t \right)^{-1} W_t^{\mathrm{H}} H V_t V_t^{\mathrm{H}} H^{\mathrm{H}} \right| \quad (1)$$

where $V_t = V_{\mathrm{RF}} V_D$ and $W_t = W_{\mathrm{RF}} W_D$. H is the matrix of complex channel gains from the transmit antennas of the BS to the IoV. V_t is the total precoder. W_t is the total combiner. The identity matrix with M dimensions is denoted by I_M. σ is additive white Gaussian noise. V_{RF} is the RF precoder. V_D is the digital precoder. W_{RF} is the RF combiner. W_D is the digital combiner. In this section, we design the HB with RF chains and data streams, i.e., $N^{\mathrm{RF}} = N_s$. The hybrid configuration entails at least N_s RF chains to implement the complete DB. The HB approach is designed for $N^{\mathrm{RF}} = N_s$, may also be utilized for $N_s < N^{\mathrm{RF}} < 2N_s$. Hybrid precoding can be divided into two phases. This problem can be written in terms of Formulas (2)–(4) for transmitters and receivers.

$$\max_{V_{\mathrm{RF}}, V_D} \log_2 \left| I_M + \frac{1}{\sigma^2} H V_{\mathrm{RF}} V_D V_D^{\mathrm{H}} V_{\mathrm{RF}}^{\mathrm{H}} H^{\mathrm{H}} \right| \quad (2)$$

such that

$$\mathrm{Tr}\left(V_{\mathrm{RF}} V_D V_D^{\mathrm{H}} V_{\mathrm{RF}}^{\mathrm{H}} \right) \leqslant P \quad (3)$$

$$|V_{\mathrm{RF}}(i,j)|^2 = 1, \forall i,j \quad (4)$$

In the case of RF precoders, the closed-form solution can be found in Eq. (6). The digital precoder is demonstrated to satisfy generally $V_D V_D^{\mathrm{H}} \propto I$ independent of the value of V_{RF}.

2.2 Path loss model

This section's large-scale path loss system is explored and contrasted using outdoor and indoor data transmission[35, 36]. The single-frequency Floating-Intercept (FI) model is mentioned in Formula (5):

$$\mathrm{PL}^{\mathrm{FI}}(d) = 10 \propto \log_{10}(d) + \beta + x_\sigma^{\mathrm{FI}},\ d \geqslant 1 \quad (5)$$

where $\mathrm{PL}^{\mathrm{FI}}(d)$ denotes the path loss in dB concerning

the 3D distance (d), between the Transmitter and Receiver (Tx-Rx), $\propto$ indicates the line slope, β represents the floating intercept in dB, and x_{σ}^{FI} indicates the Shadow Factor (SF) with Standard Deviation (SD) of the large-scale signal variability received against the direct path distance. The 3rd Generation Partnership Project (3GPP) and WINNER II channel models use the FI model[37]. A physical broadcaster to the transmitted power is not considered as the model has only two parameters ($\propto$ and β).

The single-frequency Close-In (CI) model is given by Eq. (6):

$$\mathrm{PL}^{\mathrm{FI}}(f,d)(d) = \mathrm{FSPL}(f,1) + 10n\log_{10}(d) + x_{\sigma}^{\mathrm{FI}}, d \geqslant 1 \quad (6)$$

where n represents the single model parameter, the Path Loss Exponent (PLE) with $10\,n$ indicates the path loss in dB in terms of distances, d represents the distance between Tx-Rx, and $\mathrm{FSPL}(f,d) = 20\log_{10}(4\pi df/c)$, is path loss in dB at a Tx-Rx separation distance at the carrier frequency f, where c is the speed of light. Free space path loss is computed at a distance of 1−200 m (indoor (20 m, 40 m) and outdoor (140 m, 200 m)) communication for 66 GHz frequency, where a significant amount of path loss occurs in a realistic mmWave scenario for the vehicular system. An FSPL model estimates loss for the first meter, while a PLE model estimates loss over a greater distance.

3 Result Analysis and Discussion

A 66 GHz carrier frequency is used to simulate the performance of the proposed mmWave transmitter and receiver for IoVs indoor and outdoor communication. All simulation visualization is obtained with 7.68×10^{6} bit rate, the sample time is equal to the 1/bit rate. The number of message bits is 105 based on the MATLAB simulator. The proposed modelling is executed on MATLAB R2020a with Simulink 10.4 v on Windows Operating System (OS) with 8 GB RAM Core i7 CPU. The mmWave transmitter and receiver simulation model are designed on the Simulink 10.4 v and graphical representation by MATLAB coding.

This schematic proposed model of the mmWave transmitter and receiver for the IoVs uses a QPSK transmitter, transmit array, channel, receiver array, QPSK receiver, and message display, as presented in Fig. 4. A QPSK baseband transmitter encodes the message "Hello World ###". An RF transmitter features "In-phase" and "Quadrature" (IQ) modulation, mixing, amplification, and beamforming control circuits. The RF transmitter model includes noise, non-linear effects, and antenna element coupling. An ideal channel attenuates the transmitted signal using a path loss channel model based on indoor and outdoor communication distance.

An RF receiver have two narrowband receive array antennas, Signal Noise Ratio (SNR) and receiver gain, 12-bit Analog to Digital Convertor (ADC), limited dynamic range, and two root MUSIC approach for the Angle of Arrival (AoA) determination along azimuth and elevation. The carrier and frame synchronization, demodulation, and data decoding are all included in a QPSK receiver. The user can adjust the relative angle between the transmitter and receiver vehicles. A spectrum analyzer compares normalized transmitted and received signals and displays the received message. Communication systems using lower carrier frequencies suffer less propagation loss than those using mmWave.

In the present scenario, consider the indoor (20 m, 40 m) and outdoor (140 m, 200 m) communication and path loss value depending on the distance. Figure 5 shows the path loss values for a 1−200 m distance in a

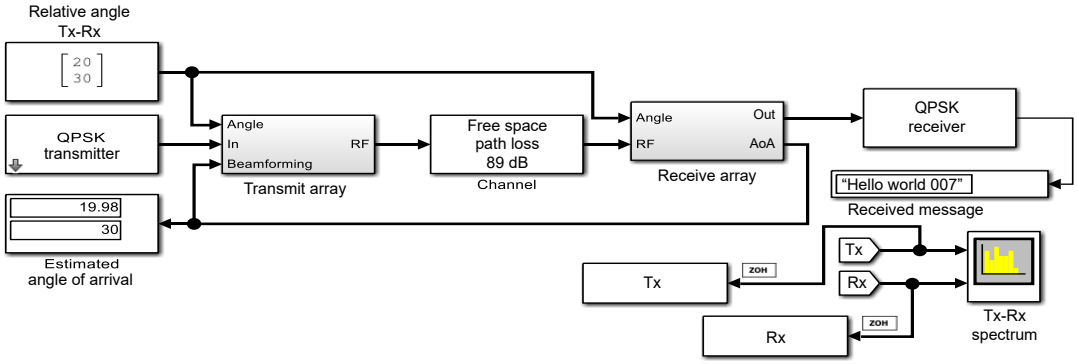

Fig. 4 mmWave transmitter and receiver simulation model. (ZOM: Zero-order hold.)

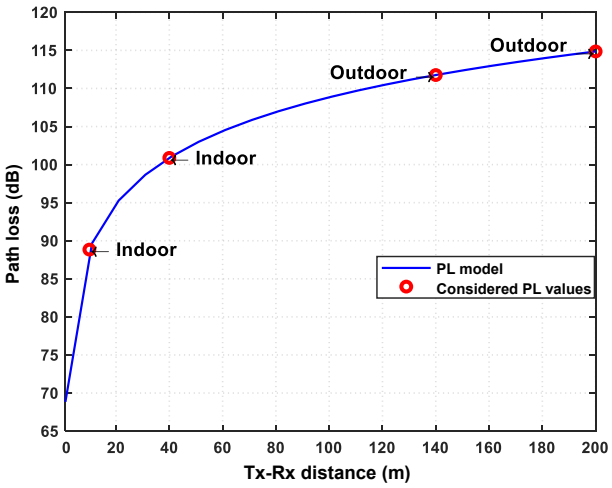

Fig. 5 Path loss model and considered path loss values for indoor and outdoor communication.

blue line, and the considered path loss values are presented by the red circle marks.

The free space path loss of the IoVs increased with increasing distance between transmitters and receivers at 66 GHz, as shown in Table 3. Path loss is caused by free-space impairments of the propagating signal, including attenuation, reflection, absorption, and refraction. The higher path of the system indicates low signal strength, receiving a signal with noise and distortion. The graphical representation of the transmitted and received power signal based on Tx-Rx distance is shown in Fig. 6.

Table 3 Path loss analysis of transmitted and received power based on Tx-Rx distance.

Distance (m)	Path loss (dB)	Transmitted power (dBm)	Received power (dBm)
20	89	0.8963	5.5802
40	101	0.8963	5.5773
140	102	0.8963	5.5758
200	115	0.8963	5.5761

Figures 7 and 8 show the transmitter and receiver power signal for indoor and outdoor communication at 66 GHz carrier frequency. It is the power measurement at the carrier frequency, across the channel, or a wide spectrum. For a better understanding of the capabilities of the proposed model, we now describe the channel characteristics for a 66 GHz channel chosen because of its high signal attenuation. These measurements are called adjacent channel power and occupied bandwidth. The center frequency and bandwidth of these channels are consistent. Transmission and reception of signal energy tend to disperse around the carrier signal frequency since communications hardware is not ideal.

We calculated the PDR and probability of the four identified errors in the simulation to validate the

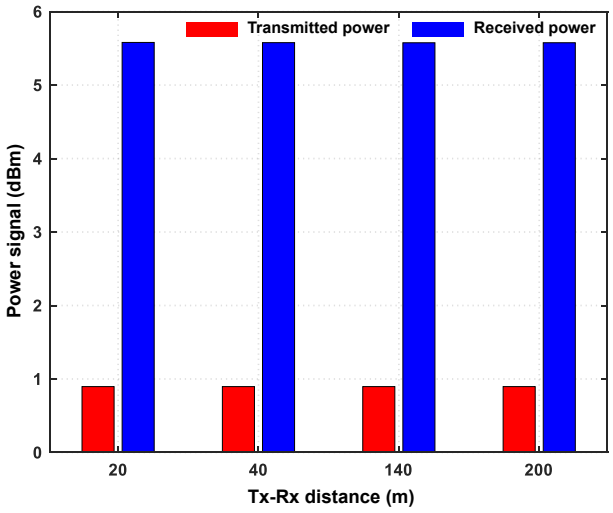

Fig. 6 Transmitted and received power signal based on the Tx-Rx distance.

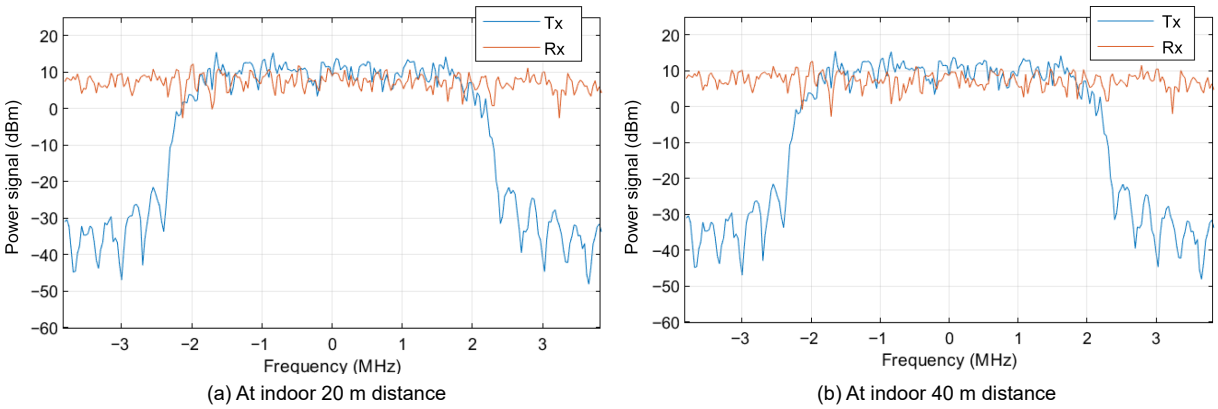

Fig. 7 Power signal of the transmitter and receiver at indoor (20 m, 40 m) distances, respectively.

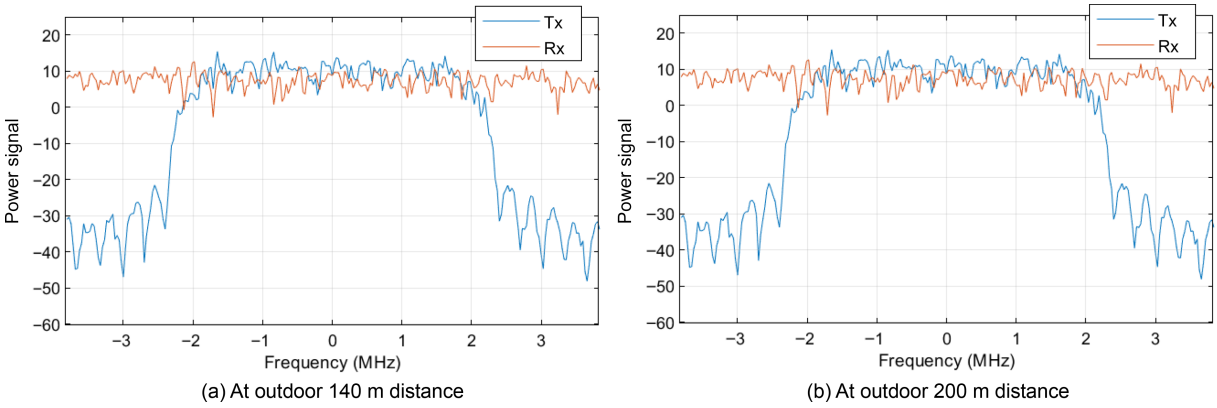

Fig. 8 Power signal of the transmitter and receiver at outdoor (140 m, 200 m) distances, respectively.

proposed models. It is accomplished by logging all packets that are correctly received and those that are not received and classifying them according to one of four error types. The distance among Tx-Rx is also included in the logs for each packet. By default, the comparison between the PDR and Packet Loss Ratio (PLR) is conducted that IoVs transmit packets with packet size $B = 256$ bytes at $\lambda = 0.0045$ Hz with a transmission power concerning the indoor and outdoor distances, as mentioned in Fig. 9.

The proposed model has also been validated for different Tx-Rx distances, path losses, packet sizes, and data rates. Figure 9 compares the PDR and PLR obtained for the Tx-Rx distances. The data rate and packet duration affect each vehicle's interference and channel load. The PDR is decreased to the indoor and outdoor distances of the IoVs, and PLR shows the performance reciprocal of the PDR.

The packet loss probability is increased with respect to the Tx-Rx distances due to the propagation effect, packet collisions, busy receiver, and sensing threshold. Figure 10 compares the probability of packet loss error by all types of transmission error acquired based on the Tx-Rx distances. Based on Fig. 10, the probability of propagation effect, sensing threshold error, and dynamic receiver error are almost perfectly matched, with only a small deviation for packet collisions. Sensing and communication ranges are affected by transmission power. The hidden terminal problem or concurrent transmissions can generate packet collisions, influencing channel load and vehicle traffic.

An analysis of the performance of 5G mmWave-based vehicular communications in indoor and outdoor scenarios is presented based on the different distances between Tx-Rx. Taking advantage of 5G communication and the proposed methodology, we can increase throughput, reduce delay, and ensure reliable transmission thanks to great improvements in our

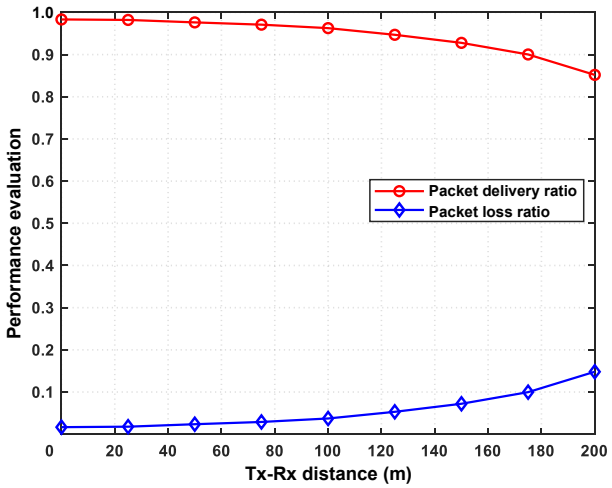

Fig. 9 Performance evaluation of the packet delivery ratio and packet loss ratio with respect to the Tx-Rx distance.

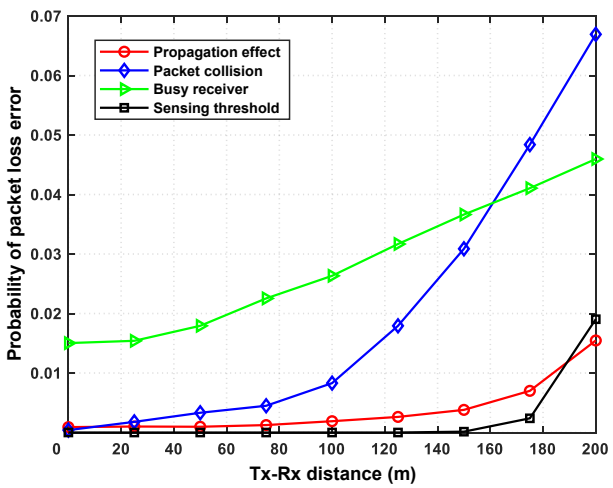

Fig. 10 Probability of packet loss error with respect to the Tx-Rx distance.

architecture. Vehicle and access point associations require a considerable amount of time, which contributes to the delay. An indicator of throughput is the rate at which messages are successfully transmitted over a communication channel. Messages containing these data may be transmitted via the IoV.

Figure 11 shows the data transmission over the Tx-Rx distance, as the distance increases between the Tx and Rx, data delivery decreases because of the high packet losses. The proposed methodology shows less delay during the connection, as shown in Fig. 12.

4 Conclusion

The IoV is becoming increasingly prevalent as autonomous vehicles and supporting infrastructure become commonplace (e.g., smart cities). This paper presents the system model of the transmitter and receiver network system and the advantages of high-frequency mmWave signal transmission for the IoV system. This work presents the mathematical modelling and simulation model of the RF signal transmit and receive system with QPSK, a 32-element hybrid beamforming antenna at 66 GHz. The performance of the transmitter and receiver is based on the indoor and outdoor distance at 66 GHz. Various simulation results analyses illustrate the performance of transmitter and receiver based on indoor and outdoor communication at 66 GHz, considering the total path loss that must be carefully addressed for V2V communication. Here, we illustrate the transmitted and received signals for indoor and outdoor communication, and it offers lower path loss exponents while simultaneously delivering a better-received message. The other performance parameters are also measured to know the data transmission behaviour between two vehicles based on the distance. The packet delivery ratio is slightly decreased for outdoor communication due to the propagation effect, packet collisions, busy receiver, and sensing threshold. With the proposed methodology, a higher packet delivery ratio and an average throughput are demonstrated with less delay during transmission. This methodology can be applied to real-time traffic or time-based IoV network data in the future.

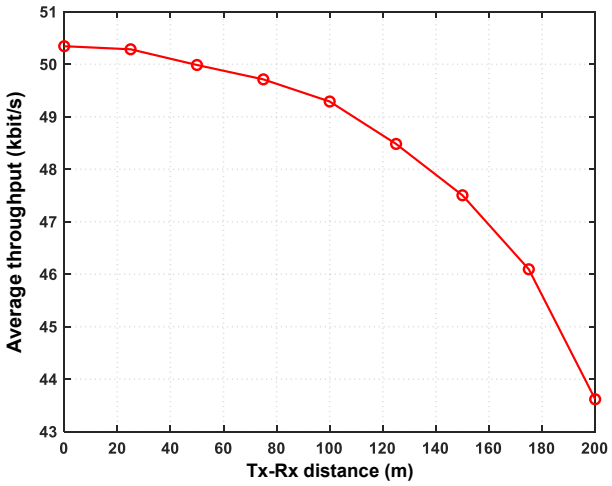

Fig. 11 Average throughput based on the Tx-Rx distance.

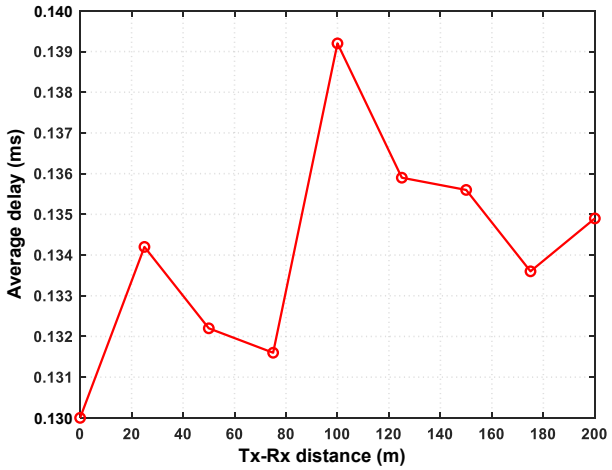

Fig. 12 Average delay based on the Tx-Rx distance.

References

[1] Z. Pi and F. Khan, An introduction to millimeter-wave mobile broadband systems, *IEEE Commun. Mag.*, vol. 49, no. 6, pp. 101–107, 2011.

[2] A. N. Uwaechia and N. M. Mahyuddin, A comprehensive survey on millimeter wave communications for fifth-generation wireless networks: Feasibility and challenges, *IEEE Access*, vol. 8, pp. 62367–62414, 2020.

[3] M. R. Akdeniz, Y. Liu, M. K. Samimi, S. Sun, S. Rangan, T. S. Rappaport, and E. Erkip, Millimeter wave channel modeling and cellular capacity evaluation, *IEEE J. Select. Areas Commun.*, vol. 32, no. 6, pp. 1164–1179, 2014.

[4] T. S. Rappaport, Y. Xing, G. R. MacCartney, A. F. Molisch, E. Mellios, and J. Zhang, Overview of millimeter wave communications for fifth-generation (5G) wireless networks—With a focus on propagation models, *IEEE Trans. Antennas Propag.*, vol. 65, no. 12, pp. 6213–6230, 2017.

[5] C. X. Wang, J. Bian, J. Sun, W. Zhang, and M. Zhang, A survey of 5G channel measurements and models, *IEEE Commun. Surv. Tutor.*, vol. 20, no. 4, pp. 3142–3168, 2018.

[6] M. Mezzavilla, M. Polese, A. Zanella, A. Dhananjay, S. Rangan, C. Kessler, T. S. Rappaport, and M. Zorzi, Public safety communications above 6 GHz: Challenges and opportunities, *IEEE Access*, vol. 6, pp. 316–329, 2018.

[7] A. M. Al-Samman, T. A. Rahman, M. H. Azmi, M. N.

Hindia, I. Khan, and E. Hanafi, Statistical modelling and characterization of experimental mm-wave indoor channels for future 5G wireless communication networks, *PLoS One*, vol. 11, no. 9, p. e0163034, 2016.

[8] S. Sun, G. R. MacCartney, and T. S. Rappaport, Millimeter-wave distance-dependent large-scale propagation measurements and path loss models for outdoor and indoor 5G systems, in *Proc. 2016 10th European Conf. Antennas and Propagation* (*EuCAP*), Davos, Switzerland, 2016, pp. 1–5.

[9] X. Zhao, S. Li, Q. Wang, M. Wang, S. Sun, and W. Hong, Channel measurements, modeling, simulation and validation at 32 GHz in outdoor microcells for 5G radio systems, *IEEE Access*, vol. 5, pp. 1062–1072, 2017.

[10] K. Zhao, C. Gustafson, Q. Liao, S. Zhang, T. Bolin, Z. Ying, and S. He, Channel characteristics and user body effects in an outdoor urban scenario at 15 and 28 GHz, *IEEE Trans. Antennas Propag.*, vol. 65, no. 12, pp. 6534–6548, 2017.

[11] M. M. Abdulwahid, O. A. S. Al-Ani, M. F. Mosleh, and R. A. Abd-Alhmeed, A comparison between different C-band and mmWave band frequencies for indoor communication, *J. Commun*., vol. 14, no. 10, pp. 892–899, 2019.

[12] F. Qamar, M. N. Hindia, T. Abbas, K. B. Dimyati, and I. S. Amiri, Investigation of QoS performance evaluation over 5G network for indoor environment at millimeter wave bands, *Int. J. Electron. Telecommun.*, vol. 65, no. 1, pp. 95–101, 2019.

[13] Z. Zhong, J. Zhao, and C. Li, Outdoor-to-indoor channel measurement and coverage analysis for 5G typical spectrums, *Int. J. Antennas Propag.*, vol. 2019, pp. 1–10, 2019.

[14] S. Song, Y. Zhu, S. Luo, J. Hou, S. Du, and Y. Song, Millimeter wave based 3D clustered MIMO channel modeling and system simulation for vehicle-to-vehicle communication, *Phys. Commun.*, vol. 40, p. 101073, 2020.

[15] I. Rasheed, An effective approach for initial access in 5G-millimeter wave-based Vehicle to Everything (V2X) communication using Improved Genetic Algorithm, *Phys. Commun.*, vol. 52, p. 101619, 2022.

[16] Z. Khan, S. M. Khan, M. Chowdhury, M. Rahman, and M. Islam, Performance evaluation of 5G millimeter-wave-based vehicular communication for connected vehicles, *IEEE Access*, vol. 10, pp. 31031–31042, 2022.

[17] K. Matrouk, Y. Trabelsi, V. Gomathy, U. Arun Kumar, C. R. Rathish, and P. Parthasarathy, Energy efficient data transmission in intelligent transportation system (ITS): Millimeter (mm wave) based routing algorithm for connected vehicles, *Optik*, vol. 273, p. 170374, 2023.

[18] Z. Zhou and M. Li, Deep reinforcement learning based edge-enabled vehicle to everything service placement for 5G millimeter wave, in *Proc. 2023 2nd Int. Conf. Networks, Communications and Information Technology*, Xining, China, 2023, pp. 138–142.

[19] P. Wu, X. Li, H. Zheng, K. Wang, J. Qin, and M. Tang, 3D modeling and analysis of cooperative perception-oriented millimeter-wave V2I networks with information value-based relay, *IEEE Trans. Veh. Technol*., vol. 72, no. 8, pp. 10505–10520, 2023.

[20] E. Benalia, S. Bitam, and A. Mellouk, Data dissemination for Internet of vehicle based on 5G communications: A survey, *Trans. Emerg. Telecommun. Technol.*, vol. 31, no. 5, p. e3881, 2020.

[21] Y. Fu, C. X. Wang, X. Mao, J. Huang, Z. Zhao, and S. McLaughlin, Spectrum-energy-economy efficiency analysis of B5G wireless communication systems with separated indoor/outdoor scenarios, *IEEE Trans. Wirel. Commun*., vol. 22, no. 12, pp. 9718–9731, 2023.

[22] L. Liang, W. Xu, and X. Dong, Low-complexity hybrid precoding in massive multiuser MIMO systems, *IEEE Wirel. Commun. Lett.*, vol. 3, no. 6, pp. 653–656, 2014.

[23] T. E. Bogale, L. B. Le, A. Haghighat, and L. Vandendorpe, On the number of RF chains and phase shifters, and scheduling design with hybrid analog–digital beamforming, *IEEE Trans. Wirel. Commun.*, vol. 15, no. 5, pp. 3311–3326, 2016.

[24] Ö. T. Demir and T. E. Tuncer, Hybrid beamforming with two bit RF phase shifters in single group multicasting, in *Proc. 2016 IEEE Int. Conf. Acoustics, Speech and Signal Processing* (*ICASSP*), Shanghai, China, 2016, pp. 3271–3275.

[25] F. Sohrabi and W. Yu, Hybrid digital and analog beamforming design for large-scale antenna arrays, *IEEE J. Sel. Top. Signal Process.*, vol. 10, no. 3, pp. 501–513, 2016.

[26] D. Zhu, B. Li, and P. Liang, A novel hybrid beamforming algorithm with unified analog beamforming by subspace construction based on partial CSI for massive MIMO-OFDM systems, *IEEE Trans. Commun.*, vol. 65, no. 2, pp. 594–607, 2017.

[27] A. Morsali, A. Haghighat, and B. Champagne, Realizing fully digital precoders in hybrid A/D architecture with minimum number of RF chains, *IEEE Commun. Lett.*, vol. 21, no. 10, pp. 2310–2313, 2017.

[28] Z. Wang, M. Li, Q. Liu, and A. L. Swindlehurst, Hybrid precoder and combiner design with low-resolution phase shifters in mmWave MIMO systems, *IEEE J. Sel. Top. Signal Process.*, vol. 12, no. 2, pp. 256–269, 2018.

[29] Y. Xiao, Y. Xiao, F. Yu, Y. Li, Y. Wang, and B. Fu, Hybrid beamforming for large-scale MIMO-OFDM in frequency selective fading, in *Proc. 2018 Int. Symp. on Networks, Computers and Communications* (*ISNCC*), Rome, Italy, 2018, pp. 1–4.

[30] S. Osman and M. M. Mowla, Low-complexity hybrid precoding analysis in 5G massive multiuser MIMO systems, in *Proc. 2019 5th Int. Conf. Advances in Electrical Engineering* (*ICAEE*), Dhaka, Bangladesh, 2019, pp. 774–777.

[31] Y. Zhang, J. Du, Y. Chen, X. Li, K. M. Rabie, and R. Kharel, Near-optimal design for hybrid beamforming in mmWave massive multi-user MIMO systems, *IEEE Access*, vol. 8, pp. 129153–129168, 2020.

[32] A. Hozouri, A. Mirzaei, S. RazaghZadeh, and D. Yousefi, An overview of VANET vehicular networks, arXiv preprint arXiv: 2309.06555, 2023.

[33] Z. Gong, F. Jiang, and C. Li, Angle domain channel

tracking with large antenna array for high mobility V2I millimeter wave communications, *IEEE J. Sel. Top. Signal Process.*, vol. 13, no. 5, pp. 1077–1089, 2019.

[34] M. A. S. Sejan and W. Y. Chung, Performance analysis of a long-range MIMO VLC system for indoor IoT, *IEEE Internet Things J.*, vol. 10, no. 8, pp. 6999–7010, 2023.

[35] G. R. MacCartney, T. S. Rappaport, S. Sun, and S. Deng, Indoor office wideband millimeter-wave propagation measurements and channel models at 28 and 73 GHz for ultra-dense 5G wireless networks, *IEEE Access*, vol. 3, pp. 2388–2424, 2015.

[36] T. S. Rappaport, G. R. MacCartney, M. K. Samimi, and S. Sun, Wideband millimeter-wave propagation measurements and channel models for future wireless communication system design, *IEEE Trans. Commun.*, vol. 63, no. 9, pp. 3029–3056, 2015.

[37] B. Mondal, T. Thomas, E. Visotsky, F. Vook, A. Ghosh, Y. H. Nam, Y. Li, J. Zhang, M. Zhang, Q. Luo, et al., 3D channel model in 3GPP, *IEEE Commun. Mag*., vol. 53, no. 3, pp. 16–23, 2015.

Rohit Sharma is an associate professor at Department of Electronics and Communication Engineering, SRM Institute of Science and Technology, India. He is an active member of ISTE, IEEE, ICS, IAENG, and IACSIT. He is an editorial board member and reviewer of more than 12 international journals and conferences, including the topmost journal *IEEE Access* and *IEEE Internet of Things Journal*. He serves as a book editor for 7 different titles to be published by CRC Press, Taylor & Francis Group, Apple Academic Press, Springer, etc. He has received the Young Researcher Award in "2nd Global Outreach Research and Education Summit & Awards 2019" hosted by Global Outreach Research & Education Association (GOREA). He is serving as a guest editor in SCI journal of Elsevier. He has actively been an organizing end of various reputed international conferences. He has served as an editor and organizing chair to the 3rd Springer International Conference on Microelectronics and Telecommunication (2019), the 2nd IEEE International Conference on Microelectronics and Telecommunication (2018), and IEEE International Conference on Microelectronics and Telecommunication (ICMETE-2016) held in India. And he has served as the technical committee member in CSMA2017, Wuhan, China; EEWC 2017, Tianjin, China; IWMSE2017, Guangzhou, China; ICG2016, Guangzhou, China; and ICCEIS2016, Dalian, China.

Preeti Rani is currently pursuing the PhD degree in wireless communication system at SRM Institute of Science and Technology, India. She received the bachelor degree in electronics & communication engineering from Raj Kumar Goel Institute of Technology for Women, Ghaziabad, India in 2012, and the MTech degree in remote sensing from Banasthali Vidyapeeth, Rajasthan, India in 2014. She obtained her one-year research from CSIR-NIO, India, in the area of satellite communication. She is serving as a reviewer of various international journals and conferences. Her interested areas of research are image processing, wireless sensor network, wireless communication, mobile ad-hoc network, vehicular ad-hoc network, Internet of Vehicles, communication network protocols, and network security.